Neoplasia • Vol. 8, No. 2, February 2006, pp. 136–142 136

www.neoplasia.com

The Role of Telomere Maintenance in the Spontaneous Growth Arrest of Pediatric Low-Grade Gliomas[1]

Uri Tabori[*,†], *Bisera Vukovic*[‡,§], *Maria Zielenska*[†,¶], *Cynthia Hawkins*[†,¶], *Ilan Braude*[§,#], *James Rutka*[†,**], *Eric Bouffet*[*,†], *Jeremy Squire*[‡,§,#] *and David Malkin*[*,†]

*Division of Hematology/Oncology, Department of Pediatrics, University of Toronto, Toronto, Ontario, Canada; †The Hospital for Sick Children, University of Toronto, Toronto, Ontario, Canada; ‡Department of Medical Biophysics, University of Toronto, Toronto, Ontario, Canada; §Ontario Cancer Institute, University of Toronto, Toronto, Ontario, Canada; ¶Department of Pediatric Laboratory Medicine, University of Toronto, Toronto, Ontario, Canada; #Department of Laboratory Medicine and Pathobiology, University of Toronto, Toronto, Ontario, Canada; **Division of Neurosurgery, Department of Surgery, University of Toronto, Toronto, Ontario, Canada

Abstract

Spontaneous tumor regression is a unique feature of pediatric low-grade gliomas (PLGG). We speculated that lack of telomere maintenance is responsible for this behavior. We first looked for evidence of telomerase activity and alternative-lengthening telomeres (ALT) in 56 PLGG. Telomerase activity was observed in 0 of 11 PLGG in contrast to 10 of 13 high-grade pediatric brain tumors. There was no ALT in 45 of 45 samples. We applied Q-FISH to eight patients whose indolent PLGG underwent two metachronous biopsies over a lag of several years. Telomere shortening was observed in the second biopsy in all tumors but not in a normal brain control ($P < .0001$), indicating that lack of telomere maintenance is associated with continuous telomere erosion. Based on these observations, we observed that younger PLGG patients who exhibit more aggressive and frequently recurrent tumors had significantly longer telomeres than older ones ($P = .00014$). Tumors with a terminal restriction fragment length of <7.5 did not recur, whereas the presence of longer telomeres (>8.0) conferred a high likelihood of late recurrences in PLGG. Our findings provide a plausible biological mechanism to explain the tendency of PLGG to exhibit growth arrest and spontaneous regression. Telomere maintenance may therefore represent the first known biologic prognostic marker in PLGG.

Neoplasia (2006) **8,** 136–142

Keywords: Telomere, telomerase, senescence, low-grade glioma, prognosis.

Introduction

Central nervous system neoplasms constitute the most common solid tumors of childhood. Although there has been great improvement in the treatment and outcome of most pediatric tumor types, this is not the case for most pediatric brain tumors (PBT). Currently, PBT are the major cause of mortality and long-term morbidity in pediatric oncology. PBT are a heterogeneous group of tumors. Some, such as high-grade gliomas, have a relentless and aggressive course. Others, such as pediatric low-grade gliomas (PLGG), exhibit erratic behavior ranging from aggressive and recurrent growth to prolonged phases of stable disease and, rarely, a striking tendency to spontaneously regress [1]. In contrast to adults, in whom low-grade gliomas tend to eventually progress or transform to high-grade gliomas [2,3], this phenomenon is extremely rare in the pediatric population, suggesting a different biologic basis. Currently, there are no plausible explanations for the tendency of certain PLGG to exhibit behaviors such as spontaneous involution. In the pediatric age group, two other potentially malignant diseases tend to spontaneously regress or arrest growth. These are stage IV_S neuroblastoma [4] and transient myeloproliferative disease (TMD) in infants with Down syndrome [5]. Recently, it has been suggested that lack of telomere maintenance in these tumors is responsible for their self-limiting nature.

Telomeres are unique structures located at the terminal ends of each chromosome. They function as a cap that protects the ends of the DNA double helix from being exposed and recognized as DNA breaks. During each mitotic cycle, a portion of the telomere is lost. Continued telomere shortening ultimately results in a growth-arrested state known as cellular senescence [6]. Telomerase is a ribonucleoprotein that catalyzes the cellular synthesis of telomeric DNA, resulting in maintenance of telomere length and increased proliferative potential. Telomerase activity is normally found only in stem cells and not in most normal somatic cells [7]. Unfortunately, more than 85% of all malignant human cancers and almost 100% of advanced cancers tested to date express high levels of

Address all correspondence to: Dr. David Malkin, Division of Hematology/Oncology, The Hospital for Sick Children, 555 University Avenue, Toronto, Ontario, Canada M5G 1X8.
E-mail: david.malkin@sickkids.ca

[1]This work is supported by a grant from BRAINCHILD Canada and The Canadian Friends of Tel-Aviv University/Hospital for Sick Children Medical Exchange Program.
Received 31 October 2005; Revised 1 December 2005; Accepted 6 December 2005.

DOI 10.1593/neo.05715

telomerase [8]. A minority of tumors utilize a different method, termed ALT, to escape senescence [9]. Telomerase is not active in TMD patients as opposed to their counterparts who evolve to acute myeloid leukemia, in which high levels of telomerase activity have been found [10]. Others have demonstrated that advanced-stage neuroblastoma exhibited significantly more telomerase activity than stage IV_S tumors [11,12]. The unpredictable behavior, spontaneous growth arrest, and regression of PLGG make them attractive candidates for the study of telomere maintenance and senescence and for possible exploitation of these features for prognostication and novel treatment options.

The primary aim of this study was to determine whether telomere maintenance is lacking in PLGG and to correlate this phenomenon with telomere shortening. A secondary objective was to utilize telomere length in PLGG as a prognostic marker for clinical use.

Methods

Tissue and Patient Accrual

Patient samples used in this study were obtained from archival biopsies of PLGG performed at The Hospital for Sick Children (Toronto, Canada) (Table 1). The study was approved by the hospital's Research Ethics Board. Protein was extracted from 11 frozen tissues of PLGG (Table 1) and 13 high-grade brain tumors for polymerase chain reaction–enzyme-linked immunosorbent assay (PCR-ELISA) telomerase assay. Although 24 patients who had had two sequential biopsies over a significant lag period were initially identified, 16 were excluded from study because they had received therapy between the two biopsies, and 2 were excluded due to lack of sufficient tissues for analysis. For telomere length assays, formalin-fixed and paraffin-embedded tissues from 16 PLGG (two sequential biopsies from each of eight patients) and two normal brain control were used for quantitative fluorescence *in situ* hybridization (Q-FISH). For each specimen, serial 5-μm sections were obtained from the blocks. Hematoxylin and eosin (H&E) staining was used to identify the regions of interest, and the same samples were used for immunohistochemistry studies. DNA was extracted from frozen tissues of a separate set of 45 PLGG for the terminal restriction fragment (TRF) assay. As noted in Table 1, each tumor sample was used only for one assay; thus, no two tests were performed on the same tumor. For prognostication and risk stratification analysis, demographic, pathological, and clinical follow-up data were obtained for PLGG patients through the neuro-oncology database and medical chart reviews.

Telomerase Assay

Tissue extraction and PCR-ELISA were performed according to the Telomerase PCR-ELISA kit (Roche Diagnostics, Mannheim, Germany), as previously described [12]. Briefly, a fragment of frozen tumor tissue was homogenized in lysis buffer and centrifuged, and the supernatant was removed. Protein concentration was determined using the Protein Assay ESL Kit (Roche Diagnostics). For each sample, a negative control was created by incubation with RNase at 37°C for 20 minutes. To identify false-negative tumor samples, a spiked sample containing both tumor lysate and positive control was also created for each specimen. The test positive control consisted of 2 μl of supplied positive control solution; the test negative control consisted of 5 μl of lysis buffer added to the reaction mixture. These samples were then incubated at 25°C. Next, telomerase was inactivated by heat treatment, and the reaction mixtures then underwent 30 PCR cycles of 94°C for 30 seconds, 50°C for 30 seconds, and 72°C for 90 seconds. On completion of the PCR protocol, denaturation and hybridization were performed according to the kit protocol. The samples were read on a Titretek Multiskan MCC/340 microtiter plate reader at 450 nm with a reference wavelength of 690 nm. Test results were expressed as the $A_{450\ nm}$ against the blank ($A_{690\ nm}$). The test negative control was accepted if the maximum absorbance $A_{450-690\ nm} = 0.25$. The test positive control was considered valid if absorbance was $A_{450-690\ nm} \geq 1.5$. Samples were regarded as telomerase-negative if $A_{450-690\ nm} = 0.2$. They were regarded as weakly positive if $A_{450-690\ nm} = 0.2$ to 0.5 and as strongly positive if $A_{450-690\ nm} > 0.5$. RNA quality was determined for specimens that were negative or weakly positive on telomerase assay.

Q-FISH

Q-FISH was performed using pan-telomeric and pan-centromeric peptide nucleic acid (PNA) probes on unstained 5-μm paraffin sections. Telomere $(C_3TA_2)_3$–specific and

Table 1. Distribution and Subtypes of PLGG Used for Different Assays.

Assay	Pathology	*n*	Location	Remarks
TRAP assay	Grade 1	7	Posterior fossa	13 High-grade brain tumors used as controls
	Grade 2	4		
Q-FISH + immunohistochemistry	Grade 1	16	Posterior fossa	Normal brain from epilepsy surgery
	Normal brain	2	Temporal lobe	
TRF—age groups	Grade 1	19	Posterior fossa	Equally distributed between groups
	Grade 2	6		
TRF—time to last progression	Grade 1	15	Optic pathway	Unresectable tumors
	Grade 2	2	Brainstem	
	Ganglioglioma	2	Spinal cord	
	Pleomorphic xanthoastocytoma	1		

centromere (16-mer repeat DNA)–specific probes directly labeled with Cy3 and fluorescein isothiocyanate (FITC) fluorescent dyes, respectively, were obtained from Applied Biosystems (Foster City, CA). The sequences of these are as follows: Flu-OEE-ATT-CGT-TGG-AAA-CGG-GA-EE; Flu-OEE-CAC-AAA-GAA-GTT-TCT-GAG-EE; Flu-OEE-CAG-ACA-GAA-GCA-TTC-TCA-EE; and Flu-OEE-TGC-ATT-CAA-CTC-ACA-GAG-EE. We used a standard technique for PNA FISH [13], with some modifications. Briefly, the sections were deparaffinized in xylene and dehydrated with 100% EtOH. Slides were incubated with 100 g/ml RNase in 2× SSC at 37°C for 60 minutes, washed with 2× SSC for 2 minutes, and treated with 1 M NaSCN for 8 minutes at 80°C. After washing with deionized H_2O, the sections were digested in 5 mg/ml pepsin solution in 0.6% NaCl (pH 1.5) for 10 minutes at 45°C and rinsed in 2× SSC at room temperature for 5 minutes. Slides were further treated with 0.1 M triethanolamine, rinsed with 1× PBS and 2× SSC for 10 minutes, dehydrated through an ethanol series (70%, 90%, and 100%), and air-dried. A mixture of 2 μl of the telomeric and centromeric probes was then applied to the sections to give a final probe concentration of 0.5 g/ml in each case. Coverslips were placed on areas of interest and sealed with rubber cement. Slides were denatured on a preheated block, transferred to a humidified chamber, and hybridized in the dark for 1 hour at 25°C. Coverslips were then removed, and the slides were washed in formamide solution for 15 minutes followed by three washes in Tween solution. Slides were counterstained with DAPI antifade mixture (Vectashield, Burlingame, CA) and analyzed. Only tissue sections with a hybridization efficiency of >95% were included in the study, having been previously validated and standardized by our group.

Image Capture

Regions of interest were determined on parallel H&E sections and identified on FISH slides using DAPI channel to minimize exposure in the Cy3 and FITC channels. Slides were then analyzed with a Zeiss Axiophot II epifluorescence microscope (Zeiss, Toronto, Canada) equipped with a mercury lamp and a ×100 1.4 NA oil immersion lens. Images were captured using a CCD camera and Isis FISH imaging software (Metasystems GmbH, Altlussheim, Germany). To compensate for cell thickness, three consecutive images at different focal depths (average of 1 μm separation) were stacked into a composite image used for quantitation. Bleaching effects due to repeated exposure of a selected area during image capture were assessed, and an intensity loss of 1% was found between exposures. Exposure times were optimized with respect to the intensities of telomere and centromere signals to prevent overexposure saturation of the signals in the original and stacked images. Once determined, they were kept constant for all slides per patient to ensure consistency in intensity measurements. For each slide, its paired biopsy served as a control to ensure that there would be no variation in fluorescence due to the pretreatment protocol. An average of 25 cells was examined on adjacent sections to quantify the telomeric and centromeric signals using Q-FISH on each of the 20 specimens (10 patients).

Image Analysis

Quantitative analysis of telomere/centromere signal intensities was performed on captured images and used to determine relative changes in telomere length and DNA ploidy. Original eight-bit images of each channel were exported from Metasystems GmbH into Adobe Photoshop, where cell borders were defined based on DAPI nuclear outline. Images of individual nuclei were then exported and analyzed quantitatively using ImageJ software. Quantitative analysis was performed (on a per-nucleus basis) on Cy3 and FITC images using a simple thresholding function to outline the signals. The intensities of all pixels outlined by the threshold were summed up on a per-cell basis and tabulated. Because ploidy changes are sometimes observed in PLGG, all telomere intensities were expressed as a telomeric-to-centromeric signals ratio for each nucleus. Centromeric intensities were used as a measure of gross ploidy changes. Telomeric ratios and centromeric intensities were then averaged between cells from each surgery and compared using analysis of variance (ANOVA) in Excel followed by Student-Newman-Keuls (SNK) test.

TRF Assay

Telomere lengths were determined by a TRF kit (Roche Diagnostics). Briefly, extracted DNA samples (1–2 μg of tumor DNA) were digested with the restriction enzymes *Rsa*I and *Hin*fI at 37°C for 2 hours and run on 0.8% agarose gels at 10 V for 18 hours. A biotinylated gamma DNA molecular weight marker was used as DNA length standard. High- and low-molecular-weight DNA were run as positive controls. The DNA samples were depurinated in 0.25 M HCl, denatured in 0.4 M NaOH/3 M NaCl, and transferred to a positively charged nylon membrane Hybond-N (Amersham Pharmacia Biotech, Little Chalfont, England, UK) by capillary blotting over 12 hours. The membrane was washed in saline–sodium citrate buffer. The blot was hybridized with a $(TTAGGG)^3$ telomere probe at 42°C for 3 hours and washed in 2× SSC/0.1% sodium dodecyl sulfate. Chemiluminescent detection was performed according to the Detection Kit (Roche Diagnostics). Detection was performed on an X-ray Hyperfilm ECL. To address the issue of tissue heterogeneity, mean TRF lengths were calculated as $\varepsilon(ODi)/\varepsilon(ODi/Li)$. The final number represents the mean molecular size of 36 equal intervals of telomeric smears in the range of 2 to 20 kb, as defined by DNA length standard. ODi reflects the measured intensity of luminescence in each of the 35 intervals. As reported in the literature, TRF lengths were recorded as telomere lengths.

Immunohistochemistry for TP53, Caspase-3, and p16

Five-micrometer sections were cut from the tissues used for the Q-FISH assay and mounted on positively charged microscope slides. Tissue sections were then baked overnight at 60°C, dewaxed in xylene, and hydrated with distilled water through decreasing concentrations of alcohol. Immunohistochemical procedures for antibodies against p53 (clone DO-7; Dako Cytomation, Mississauga, Canada), cleaved caspase-3 (Asp175; Cell Signaling Technology,

Table 2. Telomerase Activity, Measured by PCR-ELISA Technique, in Pediatric Low-Grade Astrocytomas and High-Grade Brain Tumors.

Tumor	Tested (*n*)	Positive (*n*)
Low-grade		
Astrocytoma	11	0
High-grade		
Anaplastic astrocytoma	4	2
PNET/medulloblastoma	7	6
Anaplastic ependymoma	2	2

Denvers, MA), and p16 (clone G175-405; BD Pharmingen, Franklin Lakes, NJ) at dilutions of 1:20, 1:25, and 1:10, respectively, were performed on Ventana NEXES autoimmunostainer (Ventana Medical Systems, Tucson, AZ) with a closed avidin–biotin complex method system using the 3,3-diaminobenzidine Ventana Detection System. All tissue sections were treated with heat-induced epitope retrieval and blocked for endogenous peroxidase and biotin. The counterstain of preference was hematoxylin. Appropriate positive and negative controls were also performed in parallel for each immunostain.

Statistical Analysis

To determine whether the reduction in telomeric signals was statistically significant, ANOVA was performed, followed by SNK test. Thirty cells were analyzed for each surgery. Each cell was recorded at three different nuclear vertical layers. The average of the ratio between telomeric and centromeric intensities was recorded. Analysis was performed per patient by comparing the first surgery to the second one. For telomere length/age analysis, Student's *t* test was applied.

Results

Lack of Telomere Maintenance in PLGG

Telomerase activity was noted in 0 of 11 PLGG, in contrast to 10 of 13 pediatric high-grade tumors ($P = .013$) (Table 2). None of the 45 samples analyzed using TRF demonstrated abnormal telomere elongation (Figure 3*B* shows eight representative samples) or a highly heterogeneous distribution of telomere length, indicating lack of ALT in PLGG. U-2OS and Saos-2 osteosarcoma cell lines were used as positive controls (data not shown).

Telomere Shortening in Progressive PLGG

To evaluate progressive telomere shortening, we used paraffin sections from biopsies of eight PLGG patients and one normal brain control who underwent two surgical procedures over a lag of several years (mean, 3.7 years; SD, 1.5 years) and in whom neither chemotherapy nor radiotherapy had been used as part of treatment. Q-FISH was applied to these samples, as previously described by our group (Figure 1) [13]. Lower telomere-to-centromere intensity ratios were found in the second tumor resection when compared with the first in all eight patients ($P < .001$) (Figure 2), indicating progressive telomere shortening over time in PLGG. In the normal brain control taken from a normal brain adjacent to lesions excised in two sequential epilepsy surgeries, no significant change in telomeric-to-centromeric ratio was noted between the first and second surgery (lag time, 4.5 years). Analysis of telomeric and centromeric intensities separately revealed a significant reduction in telomere intensities, whereas analysis of pan-centromeric probe revealed no significant changes between surgeries, indicating a lack of significant ploidy changes in these tumors (data not shown).

Immunostaining for Apoptosis and Senescence Markers in PLGG

Adult low-grade gliomas acquire abnormalities in the TP53 and p16 pathways as they progress. To define the role of these pathways and apoptosis in PLGG that persist over time, we stained the samples of the eight indolent PLGG that exhibited telomere shortening for TP53, p16, and cleaved caspase 3. A total of 18 samples was analyzed including eight primary and recurrent tumors and one normal brain control. Aberrant expression of TP53 was not noted in any of the samples. Cleaved caspase 3 showed rare cellular positivity in only 2 of 18 samples and was not expressed in normal

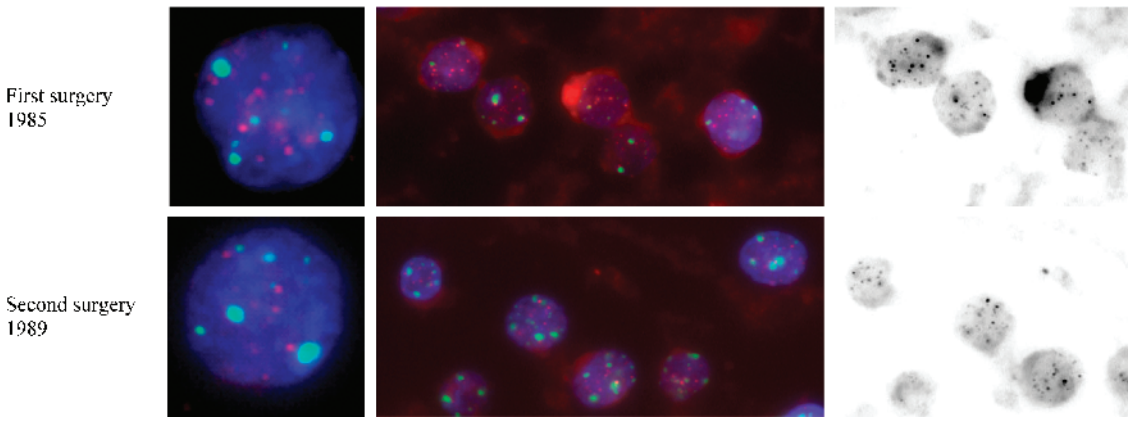

Figure 1. *Q-FISH images from two sequential biopsies of a patient with a pilocytic astrocytoma. FISH with centromeric (FITC; green) and telomeric (Cy3; red) PNA probes on paraffin-embedded recurrent PLGG. DAPI was used as a counterstain with ×100 (left) and ×10 (middle) objectives. Identical images in black and white (right) with nuclei outlined in gray and telomere signals represented by dark spots. Red dots represent telomeres, and green dots represent centromeres.*

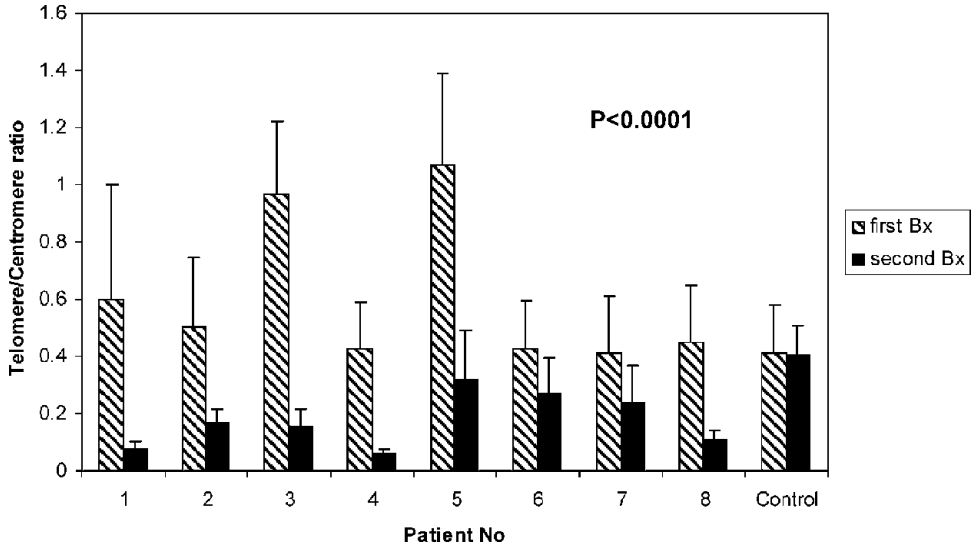

Figure 2. *Q-FISH analysis of telomere length. The y-axis represents telomere divided by centromere fluorescent intensity. Telomere intensity was reduced in the second surgery as compared to the first surgery in all patients, but not in the normal brain control. P value was calculated for 30 cells from the first tumor biopsy compared with the same number from the second tumor biopsy, per patient.*

brain controls. p16 revealed a variable degree of cytoplasmic and perinuclear staining and rare nuclear staining (1–20% of cells) in 15 of 16 tumor samples, but not in normal brain tissue (data not shown).

Telomere Length as a Prognostic Marker in PLGG

To determine the significance of telomere length as a prognostic marker in PLGG, we studied known risk groups and patients with prolonged long-term follow-up. In total, 45 PLGG were analyzed for TRF. Telomeres were longer in young patients (<4 years, n = 12) than in older ones (>10 years, n = 13) (P = .00014; Figure 3*A*), which correlates with the tendency of young patients to have a more progressive course than older ones [14,15]. Because lack of telomere maintenance may promote PLGG to senescence, we assessed the correlation between telomere length and the propensity of tumors to eventually cease growing. We measured telomere length in unresectable optic pathway, exophytic brainstem, and spinal cord PLGG cases (Table 1) who were followed for more than 2 years (mean time, 4.56 years; SD, 2.06). For each patient, time to last progression was determined as tumor survival characteristic (Figure 4). Tumors with mean telomere length (TRF) of <7.5 did not progress (n = 4). Patients with TRF of <8 did not progress more than 2 years after diagnosis (n = 5), whereas tumors with longer telomeres (n = 11) continued to progress up to 7 years from diagnosis. These findings further reinforce the correlation between continuous telomere erosion and spontaneous senescence in PLGG.

Discussion

Tumorigenesis is associated with acquisition of an immortal phenotype that requires telomere maintenance [16]. Several other alterations in cell regulation can cause malignant transformation. However, to sustain the ability to continue indefinite proliferation, cancer cells must reactivate telomerase or utilize ALT. Lack of this ability will not permit a fully malignant phenotype. Although this mechanism has been

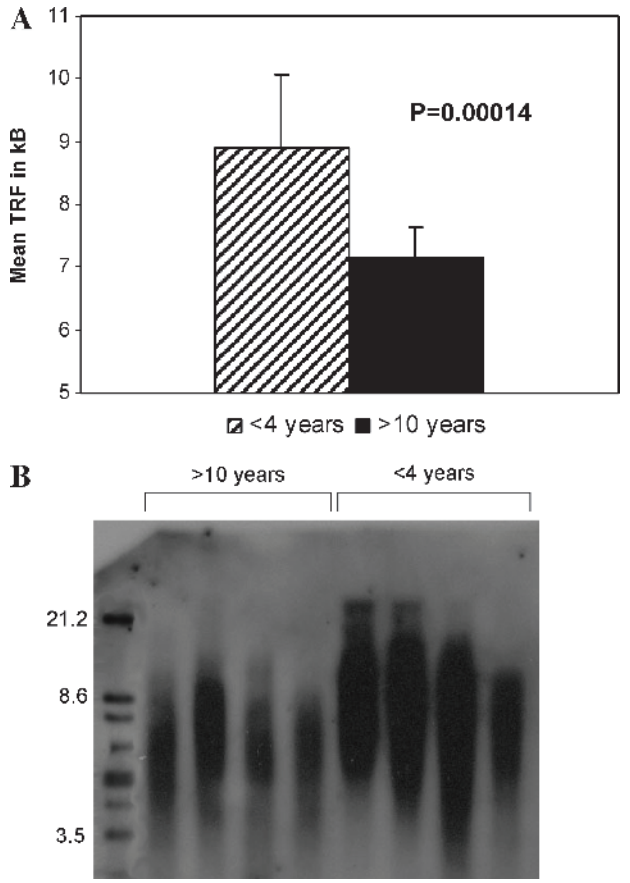

Figure 3. *TRF measurement for subgroups of PLGG patients. (A) Mean TRF length in patients younger than 4 years (n = 12) and older than 10 years (n = 13). (B) TRF analysis of PLGG in younger and older patients. Note the longer mean TRF for younger patients.*

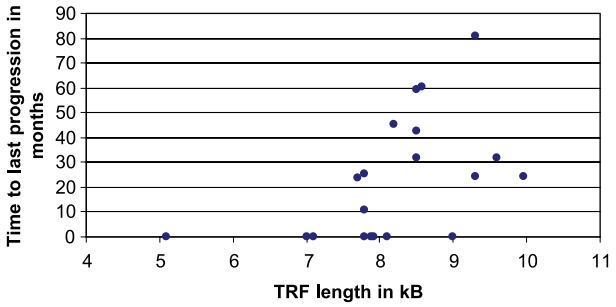

Figure 4. *Time to last progression as a function of TRF length. Patients who did not progress were designated as time to last progression = 0.*

demonstrated in laboratory *in vitro* systems, data are lacking in the clinical setting to correlate lack of telomere maintenance, telomere shortening, and clinical course.

In this study, we have shown for the first time a correlation between lack of telomere maintenance and progressive telomere shortening in pediatric tumors. Because biopsies are not performed on tumors that regress, it is impossible to prove a direct correlation between telomere erosion and senescence in active tumors. Due to their indolent course, study of the eight PLGG for which two sequential biopsies were performed enabled us to demonstrate telomere erosion over time. It is important to note that none of these patients died and that these persistent tumors were treated successfully with surgery, indicating that telomere shortening was not associated with a more biologically aggressive tumor behavior. Data from a larger set of patients in our study showed a correlation between PLGG with longer telomeres and the ability to progress for many years, as opposed to lack of progression in PLGG with shorter telomeres (Figure 4). These data further support our hypothesis.

Most cancer cells adopt mechanisms to evade cell death through alterations in major apoptotic pathways. However, senescence, if reached through progressive telomere erosion, may explain the slow growth and involution of some tumor subtypes, including PLGG. Our understanding of the role of senescence in cancer is still rudimentary. Although our observations allow us to better understand the unique clinical behavior of PLGG, they also offer a wider view of the role of telomere maintenance and senescence in tumorigenesis. Many tumors such as colon, prostate, and breast cancers are thought to originate in premalignant lesions in which telomeres are longer [13,17] and telomerase is not active. However, up to 90% of malignant neoplasms exhibit telomerase activity [8], implying that telomerase is reactivated in later stages of tumorigenesis. This feature has been shown to worsen the prognosis of glioblastomas [18,19] and colon carcinomas [20,21], whereas evidence of ALT confers better prognosis for these cancers and some pediatric sarcomas [22]. Development of approaches to prevent cells from possibly reactivating telomerase may serve as a fundamental step in the prevention of malignant transformation [23].

The striking contrast between lack of telomere maintenance and the tendency of PLGG to exhibit growth arrest, on one hand, and the relentless progression of adult LGG to high-grade tumors while reactivating their telomerase or using ALT [18,19], on the other hand, points to fundamentally different biologic mechanisms. Furthermore, lack of aberrant TP53 expression and the intact expression of p16 in PLGG suggest that these pathways are intact in PLGG as opposed to LGG in adults, where alterations in these pathways are common in the progression of LGG to high-grade astrocytomas [24,25]. p16 is involved in senescence, whereas caspase 3 is a marker for apoptosis. Therefore, expression of p16 and lack of caspase 3 expression in our indolent tumors support the role of senescence—not apoptosis—in PLGG. Although we did not look for mutations in TP53, lack of TP53 immunostaining is consistent with expression of wild-type TP53 and has been previously shown to correlate well with the presence of normal TP53 alleles and favorable outcomes in these tumors [25,26]. Therefore, our findings provide a system that might be exploited to control tumor progression in adult gliomagenesis.

As a consequence of our initial observations, in the second part of our study, we explored the use of telomere length as a prognostic marker for PLGG. Currently, there are no reliable biologic markers for predicting the behavior of these tumors. Furthermore, whereas the diagnosis of high-grade glioma carries poor prognosis, histologically similar PLGG can have different recurrence rates. Our results, therefore, are intriguing. Telomere length was significantly longer in infants and young children, a group that is generally associated with a more protracted and recurrent clinical course [14,27]. PLGG with a TRF of <7.5 did not recur or progress, whereas tumors with longer telomeres possessed the ability to progress for many years (Figure 4). The possible clinical implication of this observation is crucial because there is a trend to delay radiation therapy in these young patients by administration of chemotherapy. The ability to predict which of the tumors may spontaneously cease growing and not require radiotherapy is, therefore, imperative. These latter findings, although based on a large sample size, should be interpreted with some degree of caution because the patients were analyzed retrospectively and had undergone different treatment regimens that may have influenced outcome. Nevertheless, we believe that this observation will serve as the basis for the incorporation of these biologically relevant factors into future prospective controlled trials.

Telomere length is a novel method used to assess the risk of tumor progression and recurrence, especially when telomerase is not active. This may be true for PLGG but also for other tumors. Indeed, Gertler et al. [20] found a surprising correlation between longer telomeres and more aggressive colon carcinomas. They speculated that continued telomere erosion may not allow tumors with shorter telomeres to progress. Our results support this hypothesis by demonstrating continuous telomere shortening when there is lack of telomere stabilization by telomerase activity or ALT.

In summary, our results have three important implications. First, the correlation between lack of telomere maintenance and telomere shortening in PLGG suggests that senescence may play an important role in PLGG tumor evolution. Second, our findings support the value of telomere maintenance as an important prognostic factor in the management of

PBT. Third, PLGG can serve as a model for the emerging concept of tumor control, in which (when the tumor cell cannot be killed) its mechanisms of immortality may be disabled, making it susceptible to normal aging process, senescence, and growth arrest.

References

[1] Schmandt SM, Packer RJ, Vezina LG, and Jane J (2000). Spontaneous regression of low-grade astrocytomas in childhood. *Pediatr Neurosurg* **32,** 132–136.

[2] McCormack BM, Miller DC, Budzilovich GN, Voorhees GJ, and Ransohoff J (1992). Treatment and survival of low-grade astrocytoma in adults—1977–1988. *Neurosurgery* **31,** 636–642.

[3] Watanabe K, Sato K, Biernat W, Tachibana O, von Ammon K, Ogata N, Yonekawa Y, Kleihues P, and Ohgaki H (1997). Incidence and timing of *p53* mutations during astrocytoma progression in patients with multiple biopsies. *Clin Cancer Res* **3,** 523–530.

[4] Evans AE, Chatten J, D'Angio GJ, Gerson JM, Robinson J, and Schnaufer L (1980). A review of 17 IV-S neuroblastoma patients at the Children's Hospital of Philadelphia. *Cancer* **45,** 833–839.

[5] Zipursky A (2003). Transient leukaemia—a benign form of leukaemia in newborn infants with trisomy 21. *Br J Haematol* **120,** 930–938.

[6] Mathon NF and Lloyd AC (2001). Cell senescence and cancer. *Nat Rev Cancer* **1,** 203–213.

[7] Kim NW, Piatyszek MA, Prowse KR, Harley CB, West MD, Ho PL, Coviello GM, Wright WE, Weinrich SL, and Shay JW (1994). Specific association of human telomerase activity with immortal cells and cancer. *Science* **266,** 2011–2015.

[8] Shay JW and Bacchetti S (1997). A survey of telomerase activity in human cancer. *Eur J Cancer* **33,** 787–791.

[9] Reddel RR (2003). Alternative lengthening of telomeres, telomerase, and cancer. *Cancer Lett* **194,** 155–162.

[10] Holt SE, Brown EJ, and Zipursky A (2002). Telomerase and the benign and malignant megakaryoblastic leukemias of Down syndrome. *J Pediatr Hematol Oncol* **24,** 14–17.

[11] Poremba C, Scheel C, Hero B, Christiansen H, Schaefer KL, Nakayama J, Berthold F, Juergens H, Boecker W, and Dockhorn-Dworniczak B (2000). Telomerase activity and telomerase subunits gene expression patterns in neuroblastoma: a molecular and immunohistochemical study establishing prognostic tools for fresh-frozen and paraffin-embedded tissues. *J Clin Oncol* **18,** 2582–2592.

[12] Streutker CJ, Thorner P, Fabricius N, Weitzman S, and Zielenska M (2001). Telomerase activity as a prognostic factor in neuroblastomas. *Pediatr Dev Pathol* **4,** 62–67.

[13] Vukovic B, Park PC, Al Maghrabi J, Beheshti B, Sweet J, Evans A, Trachtenberg J, and Squire J (2003). Evidence of multifocality of telomere erosion in high-grade prostatic intraepithelial neoplasia (HPIN) and concurrent carcinoma. *Oncogene* **22,** 1978–1987.

[14] Gajjar A, Sanford RA, Heideman R, Jenkins JJ, Walter A, Li Y, Langston JW, Muhlbauer M, Boyett JM, and Kun LE (1997). Low-grade astrocytoma: a decade of experience at St. Jude Children's Research Hospital. *J Clin Oncol* **15,** 2792–2799.

[15] Khafaga Y, Hassounah M, Kandil A, Kanaan I, Allam A, El Husseiny G, Kofide A, Belal A, Al Shabanah M, Schultz H, et al. (2003). Optic gliomas: a retrospective analysis of 50 cases. *Int J Radiat Oncol Biol Phys* **56,** 807–812.

[16] Hanahan D and Weinberg RA (2000). The hallmarks of cancer. *Cell* **100,** 57–70.

[17] O'Sullivan JN, Bronner MP, Brentnall TA, Finley JC, Shen WT, Emerson S, Emond MJ, Gollahon KA, Moskovitz AH, Crispin DA, et al. (2002). Chromosomal instability in ulcerative colitis is related to telomere shortening. *Nat Genet* **32,** 280–284.

[18] Fukushima T, Yoshino A, Katayama Y, Watanabe T, Kusama K, and Moro I (2002). Prediction of clinical course of diffusely infiltrating astrocytomas from telomerase expression and quantitated activity level. *Cancer Lett* **187,** 191–198.

[19] Hakin-Smith V, Jellinek DA, Levy D, Carroll T, Teo M, Timperley WR, McKay MJ, Reddel RR, and Royds JA (2003). Alternative lengthening of telomeres and survival in patients with glioblastoma multiforme. *Lancet* **361,** 836–838.

[20] Gertler R, Rosenberg R, Stricker D, Friederichs J, Hoos A, Werner M, Ulm K, Holzmann B, Nekarda H, and Siewert JR (2004). Telomere length and human telomerase reverse transcriptase expression as markers for progression and prognosis of colorectal carcinoma. *J Clin Oncol* **22,** 1807–1814.

[21] Tatsumoto N, Hiyama E, Murakami Y, Imamura Y, Shay JW, Matsuura Y, and Yokoyama T (2000). High telomerase activity is an independent prognostic indicator of poor outcome in colorectal cancer. *Clin Cancer Res* **6,** 2696–2701.

[22] Sanders RP, Drissi R, Billups CA, Daw NC, Valentine MB, and Dome JS (2004). Telomerase expression predicts unfavorable outcome in osteosarcoma. *J Clin Oncol* **22,** 3790–3797.

[23] Seimiya H, Muramatsu Y, Ohishi T, and Tsuruo T (2005). Tankyrase 1 as a target for telomere-directed molecular cancer therapeutics. *Cancer Cell* **7,** 25–37.

[24] Kirla R, Salminen E, Huhtala S, Nuutinen J, Talve L, Haapasalo H, and Kalim H (2000). Prognostic value of the expression of tumor suppressor genes *p53*, *p21*, *p16* and *prb*, and Ki-67 labelling in high grade astrocytomas treated with radiotherapy. *J Neuro-Oncol* **46,** 71–80.

[25] Pardo FS, Hsu DW, Zeheb R, Efird JT, Okunieff PG, and Malkin DM (2004). Mutant, wild type, or overall p53 expression: freedom from clinical progression in tumours of astrocytic lineage. *Br J Cancer* **91,** 1678–1686.

[26] Pollack IF, Finkelstein SD, Woods J, Burnham J, Holmes EJ, Hamilton RL, Yates AJ, Boyett JM, Finlay JL, and Sposto R (2002). Expression of p53 and prognosis in children with malignant gliomas. *N Engl J Med* **346,** 420–427.

[27] Khafaga Y, Hassounah M, Kandil A, Kanaan I, Allam A, El Husseiny G, Kofide A, Belal A, Al Shabanah M, Schultz H, et al. (2003). Optic gliomas: a retrospective analysis of 50 cases. *Int J Radiat Oncol Biol Phys* **56,** 807–812.